

# Partial Strength Beam-to-column Connection of Cold-formed Single Channel Section: Numerical and Experimental Study

Faisal Amsyar<sup>1\*</sup>, Cher Siang Tan<sup>1</sup>, Shahrin Mohammad<sup>2</sup>, Mahmood Md Tahir<sup>3</sup> and Hazlan Abdul Hamid<sup>1</sup>

<sup>1</sup>*School of Civil Engineering, Faculty of Engineering, Universiti Teknologi Malaysia, 81310 Skudai, Johor, Malaysia*

<sup>2</sup>*Office of Chancellery, Universiti Teknologi Malaysia, 81310 Skudai, Johor, Malaysia*

<sup>3</sup>*Institute for Smart Infrastructures and Innovative Construction, School of Civil Engineering, Faculty of Engineering, Universiti Teknologi Malaysia, 81310 Skudai, Johor, Malaysia*

A full understanding of complex structural behaviour can be developed perfectly by using the combination of experimental and numerical approach. Although the basic method to determine the moment-rotation responses of the beam-to-column CFS joints has recently established from the full-scale testing, practising the finite element modelling (FEM) nowadays could explore in-depth on the number of variables and potential failure modes. In this paper, three-dimensional (3-D) model to simulate the actual behaviour of the beam-to-column CFS joints has been proposed by using multi-purpose finite element package ABAQUS version 6.14 in order to validate analysis data against the experimental works. The approach of nonlinear material characteristics, contact and sliding between different components and adopting C3D8R solid elements are proposed in this model. A total of three (3) beam-to-column CFS connections consisting of three different types of beam depths were tested in isolation in order to observe the structural behaviour based on its strength and stiffness. Comparisons between experimental and FE analysis results in term of ultimate moment capacity have shown a good correlation with strength ratios ranging from 1.12 to 1.17. Therefore, it is possible to develop a realistic model for future parametric studies such as type and configurations of the connections.

**Keywords:** semi-rigid joint; partial strength connection; finite element analysis; moment resistance; rotational stiffness; cold-formed steel

## I. INTRODUCTION

The popularity of using cold-formed steel (CFS) in semi-rigid beam-to-column connection recently has been drastically increase in construction industry as it offers more benefits compared to the identical hot-rolled steel (HRS) application. Besides of having simple configuration in fabricating and installation, CFS has the potential to serve the cost-effective purpose due to its high strength-to-weight ratio (Tan *et al.*, 2013). However, low maturity on the study of CFS joint design has required most of the engineers to refer and do some modifications to the design codes of the HRS joint. Data obtained from the experimental full-scale tests is apparently

limited to the present knowledge of the moment-rotation characteristic study of the bolted moment CFS connections and composite joints (Lam & Fu, 2005). A full understanding of complex structural behaviour can be developed perfectly by using the combination of experimental and numerical approach (Lam & Fu, 2005). Although the basic method to determine the moment-rotation responses of the beam-to-column CFS joints has recently established from the full-scale testing, practising the finite element modelling (FEM) nowadays could explore in-depth on the number of variables and potential failure modes. Figure 1 shows the examples of three-dimensional (3-D) finite element models developed by previous researchers to study the behaviour of CFS structure.

\*Corresponding author's e-mail: famsyar2@graduate.utm.my

Since past few decades, FE analysis using the multi-purpose finite element package has been proven to be the most effective way to predict the structural behaviour of non- and composite CFS connections in terms of moment capacity and rotational stiffness. However, Amsyar *et al.* (2018) stated that there are still little investigations that have been carried out and insufficient literature review regarding the FE analysis for both composite and non-composite connections for CFS structural frames, especially to the partial strength beam-to-column CFS joints. Faridmehr *et al.* (2015) has carried out isolated joint tests to a total of 12 beam-to-column joints (T1 to T3) that consists of three different beam depths and three types of connections in order to investigate the structural behaviour of screwed beam-to-column moment connections with cold-formed steel members. Type 1 (T1) connection is a beam-to-column joint directly connected to the column with self-drilling screws, meanwhile, Type 2 (T2) connection is a joint that as the same as Type 1 (T1) but with an additional angle web cleat bracket connected to the web of the beam. Type 3 (T3) connection is the same joint as Type 1 connection but with additional brackets attached as header and seater to the beam section of the connection. Tan *et al.* (2013) has developed a series of three FE models (T1 to T3) using element type of C3D20R, 20-node quadratic brick meshing available in ABAQUS and found out that the model achieved a good agreement with the experimental results by the differences up to 7% and 9% for the initial stiffness and moment resistance of the joints, respectively.

Conducting numerical modelling to investigate the stiffness and strength behaviour of the top-seat flange-cleat connection in cold-formed double channel sections, Lee *et al.* (2013) discovered that similar pattern of moment-rotation curves has been shown from the ABAQUS analysis with the experimental and analytical prediction in Eurocode 3. In addition, Lee *et al.* (2013) stressed out that less than 35% difference for strength and 50% difference for the rotational stiffness have been shown between the comparison of numerical and experimental results. Taufik (2013) has simulated a refined 3-D finite element model of semi-rigid connection with high strength steel by using ANSYS 10.0 software aid in order to study on the bolt geometry and contact effects. In his study, Taufik (2013) concluded that the proposed FE connection model is capable to predict the

ultimate load capacity and the plastic strain pattern as the comparison between the laboratory and numerical results has shown good accuracy with differences within the range of 3-5%. Adopting three-dimensional solid elements (C3D20R, 20-node linear brick with reduced integration and hourglass control), Huei *et al.* (2012) has modelled only half of the cold-formed top-seat flange cleat connection with different beam depths of 150 mm, 200 mm and 250 mm. Huei *et al.* (2012) found out that about 18-66% difference has been shown to the strength and between 1-145% difference can be seen when the comparison between analytical BS EN 1993-1-8 calculation and FE results is being done. However, a significant and better agreement can be observed by Huei *et al.* (2012) as the results are being compared with the experimental and numerical study.

In this paper, three-dimensional (3-D) model to simulate the actual behaviour of the beam-to-column CFS joints has been proposed by using ABAQUS version 6.14 in order to validate analysis data against the experimental works so that convergence in FE analysis can be achieved and usable to represent the real behaviour of full-scale test. Good correlation can be observed from both comparisons as the strength ratio obtained is in a range of 1.12 to 1.17, and the proposed model is proven to simulate well the structural behaviour of semi-rigid beam-to-column CFS joint.

## II. THREE DIMENSIONAL FINITE ELEMENT MODEL

Three-dimensional continuum (solid) elements was created in this study using a multi-purpose finite element package ABAQUS version 6.14 to simulate the partial strength of beam-to-column CFS connections. Figure 2 shows the 3D model is fully replicating to the bolted joint specimens from the actual experimental program. The sizes of all components except for the self-drilling screws are the same as the actual laboratory work since the bolt thread is not being modelled in this study. Method of loading and constraint boundary condition assigned to the models are followed closely to those used in the tests. Plus, a modified \*STATIC, RIKS method

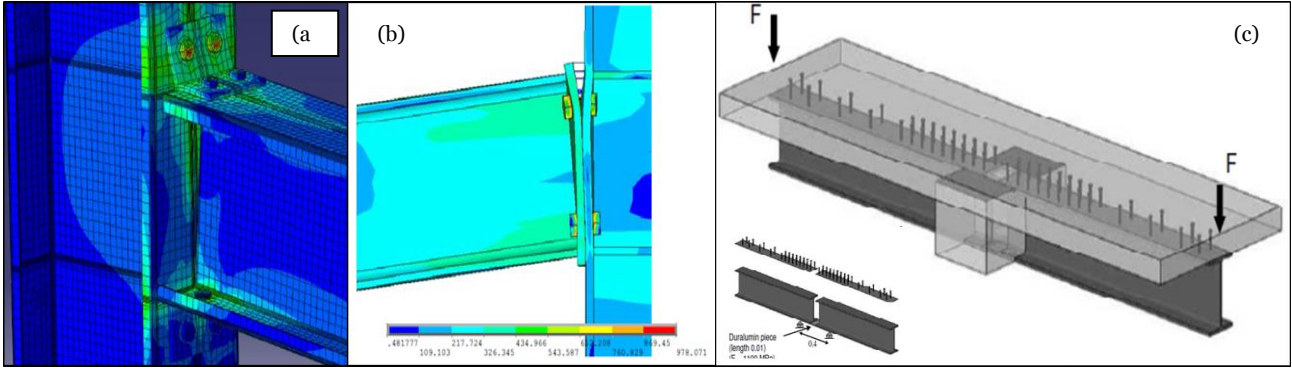


Figure 1. Examples of three-dimensional (3-D) finite element models to study the behaviour of CFS structures: (a) CFS top-seat flange cleat connection (Tan *et al.*, 2013); (b) Semi-rigid connection with high strength steel (Taufik, 2013); (c) Composite beam-to-beam joints (Guezouli *et al.*, 2014)

available in the ABAQUS library was selected to run the FE analysis, as this method can accelerate the convergence compared to the \*GENERAL, STATIC option which is difficult to achieve as there is complex interactions exist between different components in the model. The default setting of surface-to-surface contact interaction was assigned in this study to model the complex interface between the surfaces of beam-column web sections and beam-loading plate components. Finally, an eight-node linear brick, hourglass control (C3D8R) solid elements with reduced integration (1 Gauss point) has been chosen in this study to simulate all steel components.

#### A. Material Modelling – Steel Component

Stress-strain curve in terms of true stress and plastic strain was specified in the FE model for the material non-linearities. The engineering stress-strain relationship can be determined by using Equation 1 as the ABAQUS model requires the use of true stress ( $\epsilon$ ) versus plastic strain ( $\epsilon^{pl}$ ). The elastic part of the stress-strain curve was defined using \*ELASTIC option available in ABAQUS library and the \*PLASTIC option to fill up the input data of yield and ultimate strength was selected to its plastic behaviour. The plastic data defined the true yield stress of the material as a function of true plastic strain. According to Fu *et al.* (2008), the plastic strain is obtained by subtracting the elastic strain, which defined as the value of true stress divided by the Young's modulus, from the value of total strain. The relationship is written as Equation 2. The value of  $2.1 \times 10^5$  N/mm<sup>2</sup> for the Young's modulus,  $E$  and 0.3 of the Poisson's ratio,  $\nu$  were used in this study for elasticity.

$$\epsilon = \frac{F}{A} = \frac{F}{A_0} \cdot \frac{l_0}{l} = \epsilon_{nom} \left( \frac{l}{l_0} \right) = \epsilon_{nom} (1 + \epsilon_{nom}) \quad (1)$$

$$\epsilon^{pl} = \epsilon^t - \epsilon^{el} = \epsilon^t - \left( \frac{\epsilon}{E} \right) \quad (2)$$

#### B. Contact Interaction

At the initial of the observation, beam and column are assembled together by means of the self-drilling screws. However, some parts of the beam and column webs were separated as the load is applied to the structure during critical analysis. This kind of behaviour is complicated to simulate as the members are not being attached to all nodes along the boundary. To overcome this issue, small sliding formulation has been proposed as a new approach in this study to simulate all complex interactions between beam-column web surfaces and beam-loading plate interface. Using small-sliding capability available in the ABAQUS library was able to reduce the computational time during the interaction analysis between two deformable bodies or between a deformable body with rigid body in three dimensions and resulting in less simulation difference in comparison with finite sliding formulation. Property of \*HARD contact interaction from the surface-to-surface option is considered to be the most accurate option to simulate this FE model. Normal contact pressure-overclosure relationships between contact faces are chosen for the surface-to-surface interaction option by neglecting the friction factor. 'Master-slave' type algorithm was involved as the general contact formulation exists in the ABAQUS. The column web surface was defined as the 'master' surface as the element is more rigid as it is being constrained

at the upper and bottom area, meanwhile, beam and loading plate components were assigned as the 'slave' surface. Hexagon heads and screw washers were also modelled in this study as the actual size of the nominal 5.5 mm diameter of self-drilling screws. However, the details of the threads on the bolt shank were fully neglected. All bolt shanks and inner surfaces of the washers were paired up to the particular outer layer of the column and beam bolt holes and webs, respectively by using \*TIE option available in the ABAQUS library. Figure 3 illustrates the typical FE model of the beam-to-column CFS connection with adequate information on the contact interactions, load and boundary conditions.

### C. Load and Boundary Conditions

A 100×100×10 mm (10 mm thick) of pre-fabricated steel loading plate is modelled in this study as shown in Figure 4(a1) in order to apply a static concentrated load by a distance of 875 mm from the front surface of the column flanges as indicated in the actual experimental program. Modified \*STATIC, RIKS method provided in ABAQUS is applied for the increment of concentrated load. For the boundary conditions, both upper and bottom surfaces of the column components were restricted as pinned as the experimental configurations. Meanwhile, the back of the column flanges and the bottom surface of the beam flanges were restricted to z-direction so that any displacement and rotation can only be simulated simultaneously in x- and y- directions.

### D. Element Type and Meshing

An eight-node linear brick, hourglass control (C3D8R) solid elements with reduced integration (1 Gauss point) and linear 3D stress geometric order has been selected to simulate the FE model as it promises more accurate results. Suitable element sizes for different components in this model were continuously determined for the mesh sensitivity analysis and mesh convergence as well. Small approximate element size is used for the part of contact interaction area such as beam-column webs interface as it can provide accurate numerical analysis in this study. However, using a much smaller element size to the specific components must be prevented to prevent cost in computational time. Hex element shape has been selected to perform the mesh controls for all steel component except for the self-drilling

screws which are using tetra-algorithm as it was partitioned into three segments; (a) screw head, (b) washer and (c) screw shank. Figure 4(a2) shows the type of mesh control assigned to the self-drilling screws. For the beam and column members, 20 element sizes were partitioned with curvature control of maximum deviation factor of 0.1. Both pre-fabricated loading plate 1 and 2 were using 3 and 7 element sizes to mesh perfectly. Meanwhile, 5.5 mm diameter of self-drilling screws and 22 mm grade 8.8 tension bolts were meshed separately using element size of 1.5 and 2, respectively.

## III. EXPERIMENTAL STUDY

### A. Scope of Tests

A total of three (3) beam-to-column CFS connections consisting of three different types of beam depths were tested in isolation in order to observe the structural behaviour based on its strength and stiffness. Type 1 (T1) connection is used as shown in Table 1 whereas CFS beam was directly connected to the constant 250 mm depth of column section by using self-drilling screws. The variation of beam depths was assigned by 150 mm, 200 mm and 250 mm, respectively, while the depth of the column section was kept constant at 250 mm. 2 mm thick of single lipped C-section of CFS with design strength of 350 MPa was used to form up beams and columns. Table 1 (figure) illustrates all connections utilized 12 gage self-drilling screws as joint connectors where the diameter is 5.5 mm with a length of 15 mm. Figure 4(b) shows the tests were arranged to include the deformation of the components of the connections such as column flange or web, beam flange and self-drilling screw in a situation similar to an external column in a frame.

### B. Test Procedure

A full-scale testing was conducted in this study using a modified test rig and erected to accommodate beam-to-column specimen with a column height set at 3.0 m and a cantilever beam spanned at 1.0 m from the centre of the column section to the applied axial load. Figure 4(b) shows the loading frame was formed by fastening and bolting all components and subsequently anchored to the strong laboratory floor to provide pinned support at the bottom of the

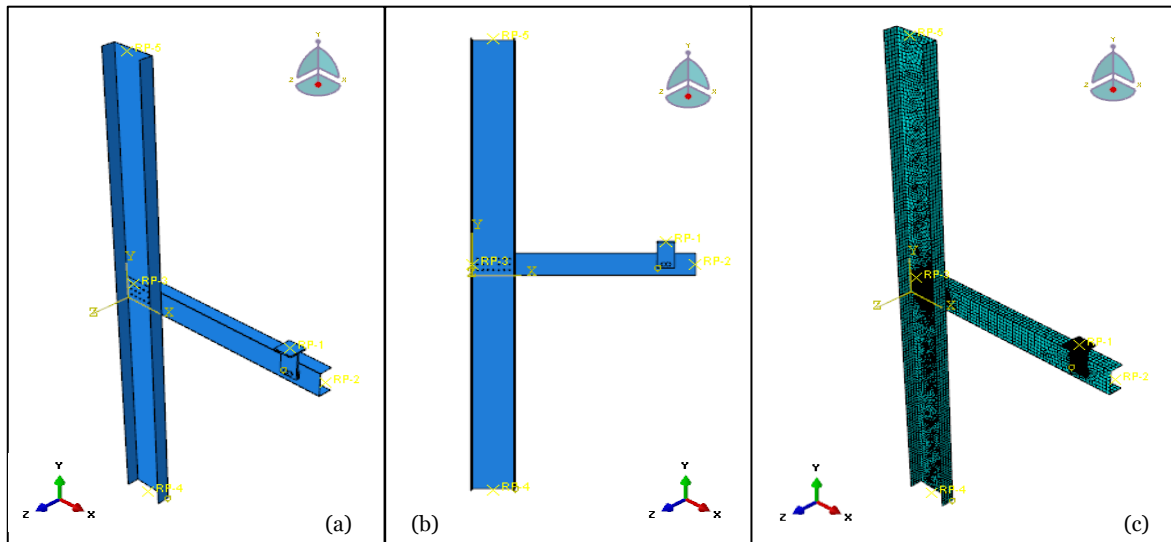


Figure 2. 3-D finite element model created using ABAQUS by replicating from the experimental program: (a) Iso view of assembling, (b) Front view model, and (c) Meshing view

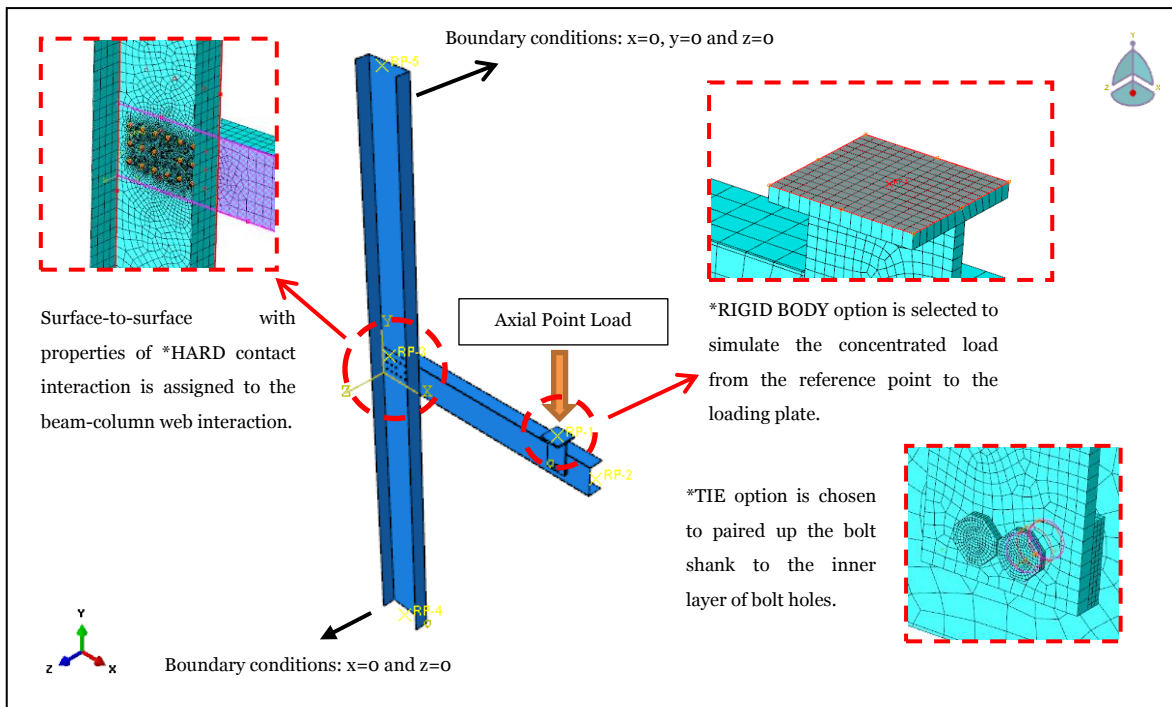
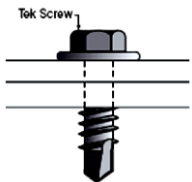
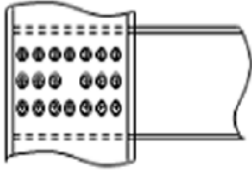


Figure 3. FE model of a typical bolted moment CFS connection with all conditions

Table 1. Configurations of isolated CFS connection tests

Type of Connector	Connection Type	Beam Depths (mm)	No of Tests
Self-drilling screws (diameter of 5.5 mm and length of 15 mm) 	Type 1 (T1) – Screws only 	150	3
		200	
		250	

column section. The height of the column is kept at 3.0 m to represent the actual height of a sub-frame column of multi-storey steel frame. The beam section is restrained from lateral movement while the column is restrained from rotation at both ends as shown in Figure 4(b). A hydraulic jack is used to apply the axial load by a distance of 875 mm from the face of the column flange in order to represent the approximate length of hogging moment that occurred on the sub-assembly steel frame. Figure 4(a1) shows a special pre-fabricated loading plate was bolted to the shear centre of the C-channel beam section to equally distribute the point load from the hydraulic jack as it can to prevent premature failure to the upper surface of the beam.

At the initial, an increment of about 2 kN was adopted in this study so that uniform data and gradual failure of the specimen can be monitored. As the significant deflection were detected during the testing, loading sequence is then controlled by the increment of deflection limited to about 5 mm as a small increment of load has resulted to substantial increase in the deflection. In this study, the tested specimens will be considered as failure when it reaches an abrupt or significant large reduction in the applied load or large rotation can be seen from the connection due to deformation of the tested specimen.

#### IV. VALIDATION OF PROPOSED MODEL

To validate the accuracy of the proposed 3-D model, FE analyses results are then compared with the laboratory test results based on the failure mechanisms and moment-rotation relationship. The proposed model is proven to be able to simulate the actual behaviour of the partial strength CFS beam-to-column connection as there is a good agreement and promising results have been achieved from both comparisons of the FEM and experimental results. Table 2 shows the overall comparison of the typical results between the laboratory and FEM analyses and the range of the strength ratio are varied from 1.12 to 1.17.

##### A. Failure Modes

As compared the FE analyses against experimental observations, the applied axial load on the tested connection for T1 specimens exert shear force combined with torsional

force. As the load nearly reached to the maximum capacity, all tested connections show large deformation with very stiff at the initial stage and followed by ductile behaviour. For a thin and lightweight material such as CFS, the common failure that always occurred is the member's local buckling. Large density of stress can be observed at the area of the beam section near to the front surface of column flanges. An obvious deformation or deflection can be seen from beam section right after the local buckling is initiated. Local buckling will limit the load capacity once it is occurred which then cause significant deformation and lowering the load carrying capacity of steel section. At the ultimate load capacity, severe failure can be captured around the connection area especially to the front flanges of column section where the beam section undergoes local buckling. The joint failed as there is a combination of shearing and tilting failures of the connected self-drilling screws. The whole set of self-drilling screws at the connection area were tilted in anti-clockwise direction. Figure 5 shows the comparisons of failure mechanisms between both experimental and FE analyses results for the beam depth of 150 mm T1 specimen. Figure 5a displayed the failure of specimen due to obvious deformation or deflection of beam section, while Figure 5b indicates that the self-drilling screws failed due to shearing as the front column of the screws undergo high stress. Figure 5c depicts the failure of connection due to tilting of self-drilling screws for both experimental and numerical observations.

##### B. Moment-rotation Responses

Plotting the moment versus rotation curve in this study is the best way to describe the typical behaviour of each type of tested T1 connection specimen through the relationship of induced moment,  $M$  and the corresponding rotation of the connection,  $\theta$ . Figure 6 shows the comparisons of experimental and FE analyses results for all models from beam depth of 150 mm to 250 mm. In both of the tests and simulation, all connections behaved a stiff initial response and then followed by the non-linear behaviour and gradually losing its stiffness with the increases of rotation. The structural analysis needs to consider this non-linearity of joint response in order to predict both stiffness and resistance accurately for a semi-continuous frame in case the joint behaviour exhibits a form of material non-linearity. Results

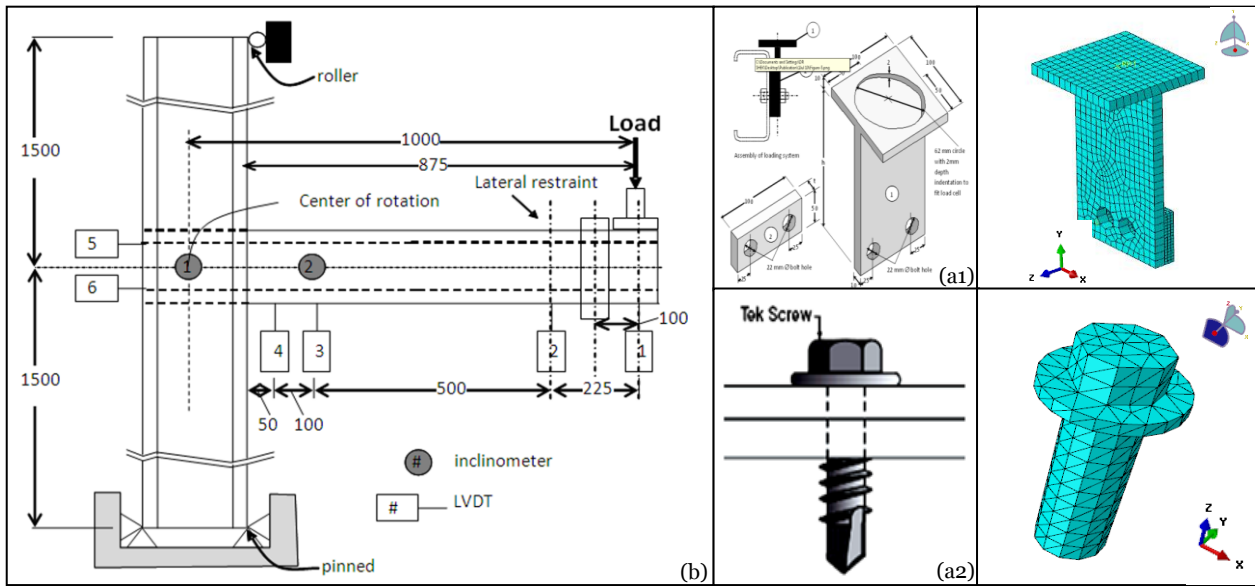


Figure 4. (a) Schematic and 3-D model views: (1) A 100×100×10 mm pre-fabricated steel loading plate is modelled using ABAQUS software; (2) Tetra-algorithm is assigned to mesh the self-drilling screws; (b) Test set-up as beam-to-external column CFS connection

show that higher initial stiffness is associated with a higher moment resistance. Due to the standard values of Young's modulus,  $E$  and Poisson's ratio,  $\nu$  are chosen as input data in 3-D modelling, numerical results seem to be slightly higher compared to the experimental in the plastic-curve behaviour. The ultimate moment resistances attained for the T1 connection specimens were 9.43 kN.m, 13.19 kN.m and 16.19 kN.m, respectively. Rotations at the ultimate moment capacities level were recorded as 20.96 mRad, 27.25 mRad and 27.30 mRad, respectively.

The initial stiffness of the connections is almost identical for all connections. The initial stiffness of the connection is mainly contributed from the resistance provided by the screws and the resistance provided by the beam. That is why the initial stiffness tends to reduce significantly as the screws started to tilt or shear off or as the connected beam and column started to deform. The results show that higher moment resistance is obtained as the depth of beam section increases. As the ultimate capacity of the connection increases, the initial stiffness of the joint specimen will proportionally be increased for both experimental and numerical results. Therefore, it can be concluded that the size of the CFS beam and column may be significantly affected the moment resistance and the rotation stiffness of the joint.

### C. Classification of Connection

From the plotted graphs of moment-rotation relationship in Figure 6, the behavioural characteristics of a particular joint and classification of the connection can be determined based on three (3) significant parameters, namely, the moment resistance (strength), initial rotational stiffness (rigidity) and rotational capacity (ductility).

In order to identify the classification of a joint, ratio of moment resistance and value of rotation capacity need to be evaluated to classify the specimen either it is in pin, rigid or semi-rigid connections. Table 3 represents the identification of connection for joint specimens. The ratio of ultimate moment resistance to the reduced moment resistance of connected beam,  $M_{max}/M_{cxr}$  ( $M_{cxr} = P_y \cdot Z_{cyr}$ ; where  $Z_{cyr}$  is the reduced elastic modulus to cater for the effects of local buckling based on Eurocode 3 Part 1.3) shows that all connections possessed maximum moment capacity more than 25% of the reduced moment resistance of the connected beam. This means that all the connections can be classified as partial strength or semi-rigid construction design. In addition, rotation capacity of all connections is in the range of 36.0 to 75.0 mRad in which the values are more than 20 mRad as suggested that the rotation capacity by Steel Construction Institute (SCI) needed to classify the connection as ductile.



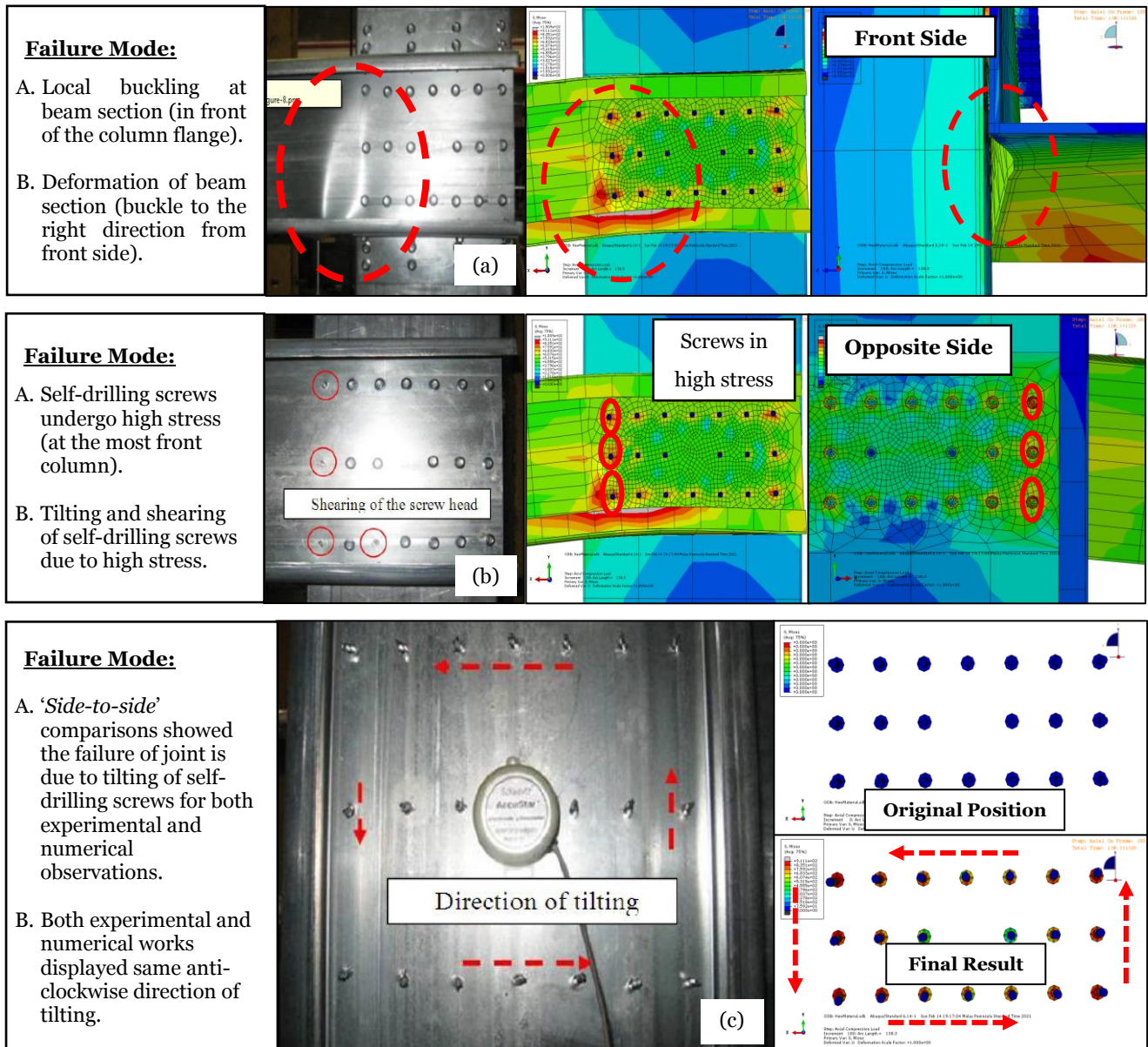


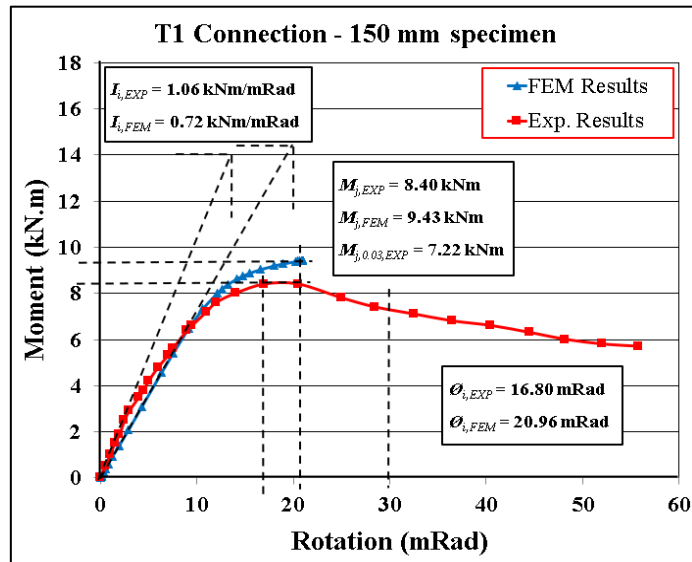
Figure 5. Failure mechanisms of T1 connection with 150 mm beam depth: (a) Failure due to the deformation of beam section and local buckling, (b) Failures due to shearing of self-drilling screws and (c) Failure of joint due to tilting of screws in anti-clockwise direction for both experimental and FE analyses

Table 2. Summary on comparisons of experimental and FE analyses results

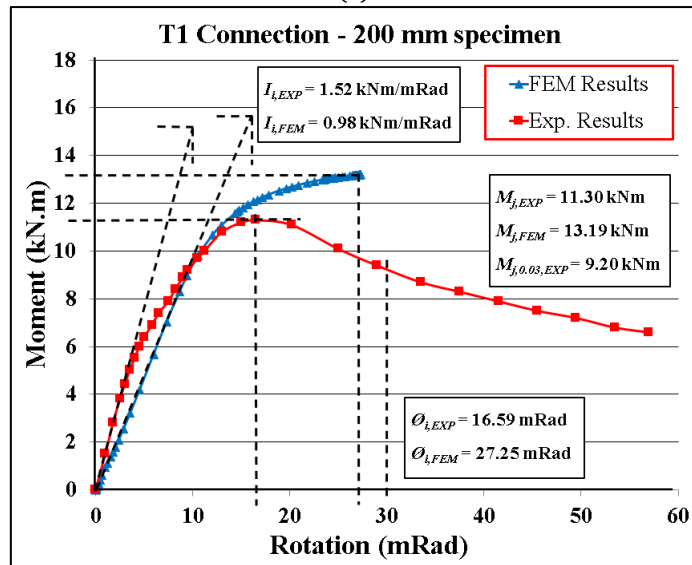
Beam Depth	Experimental Result			FEM analysis			Strength Ratio <sup>a</sup>
	Ultimate Moment Capacity, $M_{j,exp}$	Rotation capacity, $\theta_{j,exp}$ (mRad)	Initial Stiffness, $I_{j,exp}$	Ultimate Moment Resist., $M_{j,fem}$	Rotation capacity, $\theta_{j,fem}$ (mRad)	Initial Stiffness, $I_{j,fem}$	
150 mm	8.40	16.80	1.06	9.43	20.96	0.72	1.12
200 mm	11.30	16.59	1.52	13.19	27.25	0.98	1.17
250 mm	14.30	20.00	2.37	16.19	27.30	1.15	1.13

a. Strength ratio of moment resistance in this section is calculated by dividing FE analyses results to the experimental ultimate moment capacity of a connection

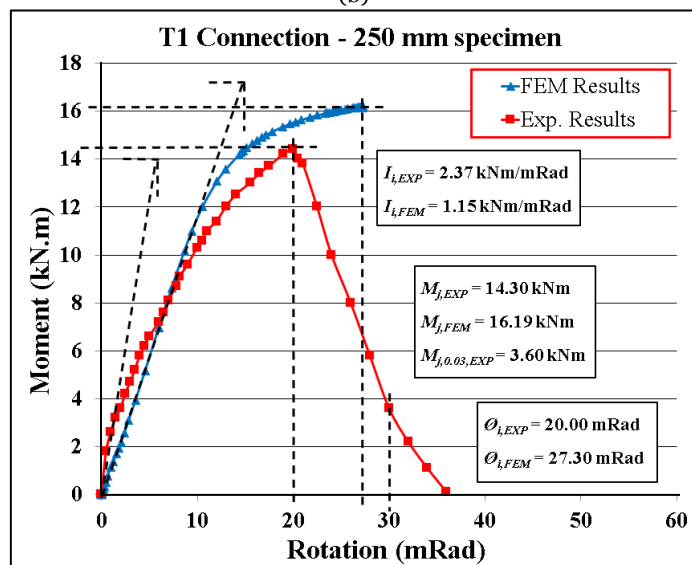




(a)



(b)



(c)

Figure 6. Comparison between experimental and FE analyses results with important information of strength, rotation and initial stiffness: (a) Specimen with beam depth 150 mm, (b) Specimen with beam depth 200 mm and (c) Specimen with beam depth 250 mm

Table 3. Classification of connection for both experimental and numerical results

Beam Depth (mm)	Experimental Result	FEM analysis	Theoretical Calculation	$M_{max}/M_{cxr}$ <sup>a</sup>	
	Ultimate Moment	Ultimate Moment	Eurocode 3: Part 1.3	Exp.	FEM
	Capacity, $M_{j,exp}$ (kN.m)	Resist., $M_{j,fem}$ (kN.m)	Moment of beam, $M_{cxr}$ (kN.m)	Result	Result
150 mm	8.40	9.43	10.60	0.80	0.89
200 mm	11.30	13.19	16.45	0.69	0.80
250 mm	14.30	16.19	22.94	0.62	0.71

a.  $M_{max}/M_{cxr}$  can be calculated by dividing the ultimate moment resistance to the reduced moment resistance of connected beam.

## V. CONCLUSION

Three-dimensional (3-D) FE model of semi-rigid beam-to-column CFS connection has been described in this paper and validation with three test specimens through the experimental program has shown that good agreement can be obtained from both outcomes. Plotted moment-rotation graphs from the analyses and tests data is focussing on the comparison of strength and stiffness of the joints. It can be concluded that in-depth analysis on the structural behaviour of partial strength CFS connection can be performed obviously from the FE method as it is difficult to measure via physical tests, such as complex interactions between surfaces and the principal stress in the connection. Comparisons between experimental and FE analysis results in term of ultimate moment resistance have shown a good correlation with strength ratios ranging from 1.12 to 1.17. Since all

connections possessed greater than 25% of  $M_{max}/M_{cxr}$ , it can be concluded that all joints are in partial strength connection. As the general-purpose finite element package ABAQUS has become a powerful tool to understand the fundamental behaviour of the CFS joints, it is possible to develop a realistic model for future parametric studies. A complete analytical design procedure and necessary recommendations can be proposed by consistently using the finite element studies as indicated in the component method of steel joint design in Eurocode 3.

## VI. ACKNOWLEDGMENT

The authors would like to express their utmost gratitude to the financial and technical contribution by the Malaysia Ministry of Education (MOE) and Universiti Teknologi Malaysia (Grant 17H53, Grant 21H68 and Grant 21H47).

## VII. REFERENCES

- Amsyar, F, Tan, CS, Ma, CK & Sulaiman, A 2018, 'Review on composite joints for cold-formed steel structures', E3S Web of Conferences, vol. 65, pp. 1-11.
- Faridmehr, I, Tahir, MM, Osman, MH, Nejad, AF & Hodjati, R 2015, 'An experimental investigation of stiffened cold-formed c-channels in pure bending and primarily shear conditions', Thin-Walled Structures, vol. 96, pp. 39-48.
- Fu, F, Lam, D & Ye, J 2008, 'Modelling semi-rigid composite joints with precast hollowcore slabs in hogging moment region', Journal of Constructional Steel Research, vol. 64, pp. 1408-1419.
- Guezouli, S, Somja, H, Kiang, SS & Lachal, A 2014, 'Numerical modelling of composite beam-to-beam joints- innovative solutions', American Society of Civil Engineers, pp. 542-553.
- Huei, LY, Siang, TC, Tahir, MM & Mohammad, S 2012, 'Numerical modelling and validation of light gauge steel top-seat flange-bleat connection', Journal of Vibroengineering, vol. 14, no. 3, pp. 1104-1112.
- Lam, D & Fu, F 2005, 'Modelling of semi-rigid composite beam-column connections with precast hollowcore slabs', Advances in Steel Structures, vol. 1, pp. 787-792.
- Lee, YH, Tan, CS, Lee, YL, Tahir, MM, Mohammad, S & Shek, PN 2013, 'Numerical modelling of stiffness and strength behaviour of top-seat flange-bleat connection for cold-formed double channel section', Applied Mechanics and Materials, vol. 284-287, pp. 1426-1430.

- Lee, YH, Tan, CS, Mohammad, S, Lim, JBP & Johnston, R 2015, 'Numerical study of joint behaviour for top-seat flange cleat connection in cold-formed steel structures', *Scientia Iranica*, vol. 22, no. 4, pp. 1554-1566.
- Tan, CS, Lee, YH, Lee, YL, Mohammad, S, Sulaiman, A, Tahir, MM & Shek, PN 2013, 'Numerical simulation of col-formed steel top-seat flange cleat connection', *Jurnal Teknologi*, vol. 66, no. 3, pp. 63-71.
- Taufik, S 2013, 'Numerical modelling of semi-rigid connection with high strength steel', *Study of Civil Engineering and Architecture (SCEA)*, vol. 2, no. 2, pp. 36-47.